CRYSTAL GROWTH & DESIGN

Article

pubs.acs.org/crystal

Solid-State Supramolecular Chemistry of a Benzylpyridine-Functionalized Zwitterion: Polymorphism, Interconversion, and Porosity

Leigh Loots, James P. O'Connor, Tanya le Roex, and Delia A. Haynes*

Department of Chemistry and Polymer Science, Stellenbosch University, Private Bag X1, Matieland, 7602, Republic of South Africa

Supporting Information

ABSTRACT: The reaction between acetylenedicarboxylic acid and 4-benzylpyridine yields two products: a salt and a zwitterion. The relationship between these two products has been investigated, revealing that the salt is the kinetic product of the reaction and the zwitterion is the thermodynamic product. The zwitterion has four polymorphs and three solvates. Interconversion between these forms has been studied and was shown to be solvent-mediated when it occurs; conversion between most polymorphic forms cannot be achieved using thermal methods. The temperature at which the reaction to form the zwitterion is carried out and the solvent system used are crucial in determining which polymorphic form crystallizes from the reaction. In addition, polymorphic Form I is shown to be porous to dioxane.

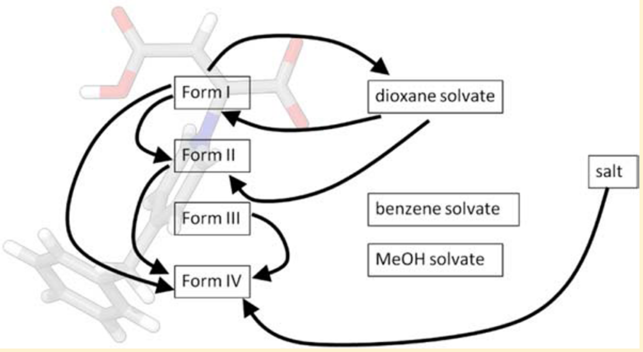

INTRODUCTION

The occurrence of multiple solid-state forms, including polymorphs and solvates, is a subject of great interest to solid-state chemists. A number of reasons have been proposed as to why particular molecules might exhibit multiple forms in the solid state. It has been suggested that conformational flexibility is a significant factor when considering the possibility of molecules manifesting in different solid-state forms (polymorphs, hydrates, solvates, etc.),[1−3] as flexible molecules make use of multiple pathways of self-organization or self-assembly.[4] Different crystallization conditions, such as solvent, temperature, and humidity, as well as the crystallization method (cooling, slow evaporation, from a melt or by sublimation) can influence the formation of different polymorphs.[5] Because molecules tend to close-pack in the solid state, structural flexibility and bulky substituents can also affect the solid-state behavior of a molecule.[6] Awkwardly shaped molecules have more difficulty packing efficiently, and this can lead to polymorphism, guest inclusion, void space, or porosity in the resulting crystal structure.

Porosity can be "engineered" by designing framework materials such as metal−organic framework (MOFs) or covalent−organic framework (COFs) materials, which employ coordination or covalent bonds, respectively, to construct the framework. Hydrogen-bonded organic framework materials are relative newcomers to the field of porosity, first introduced by Wuest[7−9] and co-workers. Ward[10−15] and co-workers followed soon after with a series of guanidinium sulfonate framework materials that show potential in second-order harmonic generation and nonlinear optical properties due to polar ordering of the included guest molecules. These materials are interesting in part because they are salts: porous solids based on ionic organic materials are of interest due to the combination of strong and directional charge-assisted hydrogen bonds with the flexibility, in terms of dissolution and recrystallization, offered by organic systems. A series of diamondoid porous organic salts constructed from triphenylmethylamine and various sulfonic acids was reported by Tohnai[16−19] and co-workers. These compounds "breathe" in order to exchange guest molecules, and it was shown that a tunable fluorescent response to various absorbed guests could be achieved when using a fluorescent sulfonic acid in the structure. Our research group has also published work on porous salts based on the pamoate ion,[6,20] which have been shown to be porous or highly selective to certain guest molecules.

Recently, we reported the synthesis and crystallographic analysis of a series of pyridyl-derived zwitterionic compounds.[21] The synthesis of these zwitterions is simple, employing mild conditions where the products are obtained as single crystals without further purification. Exploring the potential of these compounds as supramolecular building blocks is highly appealing: all of the zwitterions have several hydrogen-bond donors and acceptors that, due to the unusual shapes of the molecules, are positioned to form extended hydrogen-bonded chains or networks. Due to the awkward shape and strong hydrogen-bonding potential of these zwitterions, we anticipated

Received: August 26, 2015
Revised: October 23, 2015

DOI: 10.1021/acs.cgd.5b01238
Cryst. Growth Des. XXXX, XXX, XXX−XXX

Scheme 1. Synthesis of Zwitterion 1 and Salt 2

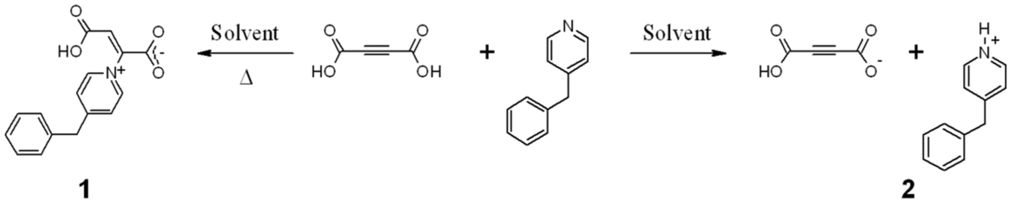

Table 1. Selected Crystallographic Data for the Different Forms and Solvates of 1 as well as for Salt 2

structure	Form I	Form II[21]	Form III	Form IV	$\mathbf{1}_{\mathrm{Diox}}$	$\mathbf{1}_{\mathrm{Benz}}$	$\mathbf{1}_{\mathrm{MeOH}}$	salt (**2**)
crystallization solvent	THF or acetone	$\mathbf{1}_{\mathrm{Diox}}$ immersed in MeOH/H_2O	acetone/*p*-xylene	water (recryst.)	dioxane	benzene/MeOH	CH_2Cl_2/MeOH	MeCN
formula weight	283.27	283.27	283.27	282.28	327.32	322.33	292.20	226.25
crystal symmetry	monoclinic	orthorhombic	monoclinic	orthorhombic	monoclinic	monoclinic	monoclinic	monoclinic
space group	$P2_1/n$	*Pbca*	$P2_1/c$	*Pbca*	$P2_1/n$	$P2_1/n$	$P2_1/n$	$P2_1/n$
a (Å)	13.801 (5)	15.143 (1)	8.197 (3)	8.661 (2)	13.882 (2)	13.870 (4)	13.935 (1)	5.390 (3)
b (Å)	7.407 (3)	7.687 (1)	6.208 (2)	8.262 (2)	7.442 (1)	7.451 (2)	7.410 (1)	8.680 (4)
c (Å)	14.537 (6)	22.303 (2)	26.752 (9)	36.966 (8)	15.134 (3)	15.204 (4)	14.532 (1)	25.258 (1)
α (deg)	90	90	90	90	90	90	90	90
β (deg)	97.369 (6)	90	92.374 (4)	90	96.588 (2)	96.399 (4)	97.066 (1)	95.143 (7)
γ (deg)	90	90	90	90	90	90	90	90
Z	4	8	4	8	4	4	4	4
V (Å^3)	1473.8 (1)	2596.1 (3)	1360.1 (8)	2645.1 (9)	1553.1 (5)	1561.5 (7)	1.489.2 (2)	1176.9 (1)
temp. (K)	100 (2)	100 (2)	100 (2)	296 (2)	100 (2)	100 (2)	100 (2)	296 (2)
D_{calcd} (g·cm^{-1})	1.277	1.450	1.383	1.423	1.400	1.371	1.300	1.277
N_{total}	8972	15 206	8231	11 543	9203	9242	32 614	7165
N_{ind}	3392	3070	3102	2385	3569	3523	3407	2648
N_{obsd}	2857	2711	2325	1521	2930	1989	2794	1776
R_1 [$I > 2\alpha(I)$]	0.042	0.0379	0.0437	0.0592	0.0485	0.0617	0.0465	0.0444
R_{int}	0.0285	0.0222	0.0379	0.0656	0.0224	0.0695	0.0390	0.0233
wR_2	0.1053	0.0973	0.0939	0.1305	0.1234	0.1418	0.1231	0.1082
GOF	1.038	1.019	1.055	1.051	1.045	1.037	1.045	1.036
μ (mm^{-1})	0.093	0.105	0.100	0.103	0.103	0.097	0.095	0.086
void volume[a] (Å^3)	21.3 (1.5)/ 28.7 (1.4)	N/A	N/A	N/A	146.2 (1.5)/ 151.7 (1.4)	146.8 (1.5)/ 151.195 (1.4)	24.44 (1.5)/ 68.78 (1.4)[b]	N/A
Squeeze[28] (1.2 Å probe) (void volume, electrons per void)	65 Å; 3 e	N/A	N/A	N/A	145 Å; 44 e	142 Å; 40 e	58 Å; 11 e	N/A

[a] Void volume was determined as contact surface using MSRoll;[29] probe radius, in angstroms, is given in parentheses. For solvates, this is the volume of the void if the solvent is deleted, in other words, the volume of the space occupied by the solvent. [b] Void volume was calculated using the averaged structure of the disorder model.

that they might prove to be good building blocks for organic hosts or porous materials. It also seemed possible that they would exhibit a variety of solid-state forms. Polymorphism in zwitterionic systems has been investigated previously, with the majority of these studies focusing on drug compounds or amino acids.[22−27]

Several of the zwitterions reported in our previous study[21] have been further investigated, and, in this article, we report the detailed study of (2*Z*)-2-(4-benzylpyridinium-1-yl)-3-carboxy-1-hydroxyprop-2-en-1-olate, **1** (Scheme 1).

The synthesis of **1** proceeds via reaction of acetylenedicarboxylic acid (ADC) and 4-benzylpyridine (4BP) in solution. Our previous study briefly reported three forms for **1**: two polymorphs and a dioxane solvate. The crystal structure of one of the polymorphs was also described (CCDC refcode BIXNON no. 987549).[21] Further investigation of this zwitterion in the solid state has yielded interesting solvent inclusion as well as polymorphic behavior. A related salt, **2**, was also obtained from the same starting materials. To date, three solvates (1,4-dioxane, benzene, and MeOH) and four polymorphic forms of **1** have been obtained from solution crystallization methods. (We have used the term polymorphs to describe these four forms despite the fact that some contain the cis isomer of the molecule and some contain the trans isomer. We have observed solvent-mediated conversion between a cis-containing form and a trans-containing form, so the term polymorphs is applicable.) This article describes these forms, as well as the investigation of the relationships between them. In addition to an analysis of the structures of the various forms of zwitterion **1** and the relationships between these forms, we also report the characterization of a new ionic hydrogen-bonded porous material, Form I of **1**. As discussed above, the only porous ionic materials reported in the literature to date are the diamondoid porous organic salts (dPOS) reported by Tohnai[16−19] and the porous pamoate salts reported by our group.[6,20] Form I of **1** is thus a rare example of a porous ionic organic material.

RESULTS AND DISCUSSION

Zwitterion **1** is synthesized by direct reaction of the starting materials in solution (Scheme 1). Crystal structures of several forms of **1** have been obtained, as well as the crystal structure of salt **2**. Crystallographic data are summarized in Table 1, and hydrogen-bonding distances and angles are tabulated in the Supporting Information. To date, zwitterion **1** has been shown to crystallize in four different polymorphic modifications, depending on the reaction solvent (Table 1 and Experimental Section). Three of these polymorphs contain the zwitterion in the trans conformation (Figure 1a); one contains the cis isomer (Figure 1b). One of these, herein Form II, has been described in detail previously,[21] but it will be discussed briefly here for comparative purposes. The crystal structures of **1** and its solvates, as well as salt **2**, are described first. This is followed by a discussion of the relationship between the zwitterion and the salt and then a description of investigations into conversion between the different solid state forms.

It is important to note that **1** is insoluble in most organic solvents; thus, most of the products reported crystallize directly from the reaction mixture and have not been recrystallized.

Polymorphs of 1. Form I of zwitterion **1** crystallizes from acetone or tetrahydrofuran in space group $P2_1/n$, with one molecule of **1** in the trans conformation in the asymmetric unit (Figure 1a). Hydrogen-bonded chains of molecules interdigitate in a herringbone pattern (Figure 2). The benzylpyridine moieties are twisted and bent at the methylene bridge, with a dihedral angle of 79.87(7)° between the two ring planes (angle at methylene = 114.01°).

A notable and unusual feature of Form I is the small pockets of open space in the structure, which have a volume of 21.3 Å^3 when using a probe with radius 1.5 Å (Figure 2b). This is reflected in the lower calculated density of Form I (Table 1). Thermogravimetric analysis (TGA) and Squeeze[28] results have confirmed that the voids are empty (see Supporting Information). It is very unusual for there to be open space within a crystal structure, and this is especially interesting since three close-packed polymorphs of **1** have been obtained under very similar conditions (vide infra). Of further interest is the fact that this open form appears to be quite stable under atmospheric conditions; it can be left under ambient conditions on the open bench for at least 6 days without any observable change in form (some samples have been kept on the open bench for up to a year without any observable change in structure or evidence of conversion to any of the other solid-state forms).

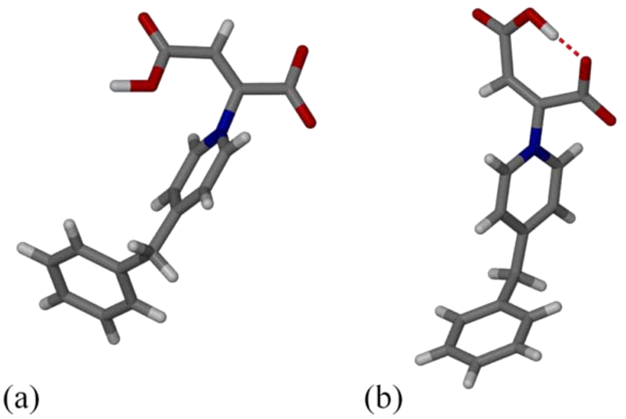

Figure 1. (a) Trans isomer of **1**, as seen in Form I. (b) Cis isomer of **1**, as seen in Form III.

Form II[21] of zwitterion **1** crystallizes in orthorhombic space group *Pbca*, with one zwitterion in the trans conformation in the asymmetric unit. As in Form I, the zwitterions hydrogen bond to one another via the carboxylate moieties to form one-dimensional chains. Two such chains are positioned alongside one another in a slightly offset fashion. These pairs of chains stack one on top of another along [001] to form bilayers, which are then stacked antiparallel with one another along [100] (Figure 3).

Form III crystallizes in monoclinic space group $P2_1/c$, with one molecule of **1** in the cis conformation (Figure 1b) in the asymmetric unit. There is no intermolecular hydrogen bonding in this structure, there are only intramolecular hydrogen bonds between the carboxylic acid and carboxylate moieties, which arise due to the cis conformation of the alkene moiety. The pyridyl and phenyl rings in each molecule are twisted so as to be approximately perpendicular to one another. Molecules pack alongside one another such that the ionic groups stack and the phenyl groups stack. This results in hydrophobic and hydrophilic bands in the structure (Figure 4).

Reactions to synthesize **1** also often yield a fourth polymorph, Form IV. This form is obtained from reactions in MeOH, despite the existence of a MeOH solvate (vide infra), which was obtained once from a DCM/MeOH mixture. Microanalysis, NMR, and mass spectrometry confirmed that Form IV contained zwitterion **1**; this was necessary due to the difficulty experienced in obtaining single crystals of this form.

Single crystals of Form IV were eventually obtained by recrystallization of the powdered product (obtained by reaction in MeOH) from water. This form crystallizes in orthorhombic space group *Pbca*, with one molecule of **1** in the asymmetric unit. The zwitterion is in the trans conformation, as in Forms I and II; however, the hydrogen-bonding motif is considerably different. The hydrogen bonds between the carboxylate and carboxylic acid moieties have an angle that is quite different, resulting in a zigzag chain with the benzylpyridine moieties projecting outward. The chains pack one on top of another in an offset manner. The phenyl moieties of neighboring chains interdigitate to form a herringbone motif. The molecules of **1** are bent at the methylene bridge (113.1°), with a dihedral angle of 69.28(8)° between the pyridyl and phenyl rings (Figure 5).

Solvates of 1. To date, three solvates of **1** have been characterized. Two of these (the dioxane and benzene solvates) are isostructural to one another and bear a close relationship to Form I of **1** (the open form). The methanol solvate is isostructural to Form I, but it contains MeOH in the voids.

$\mathbf{1}_{\mathrm{Diox}}$ crystallizes in monoclinic space group $P2_1/n$, with one zwitterion and one-half a molecule of 1,4-dioxane in the asymmetric unit. The zwitterion is in the trans form, and the benzylpyridine moiety is bent (113.8°) at the methylene bridge such that the aromatic rings are at an angle of 58.36° to one another. Once again, one-dimensional chains are formed via hydrogen bonding between carboxylate groups. Parallel chains are arranged into layers separated by dioxane molecules (Figure 6a). The guest molecules occupy small pockets surrounded by eight molecules of **1**. Pockets were mapped with MsRoll[29] using a 1.5 Å probe radius and are approximately 146.2 Å^3 in volume. When the guest molecule is viewed along with the mapped voids, it is clear that the oxygen atoms of the 1,4-dioxane molecules are protruding out of the contact surface, indicating that there are close contacts between these atoms and

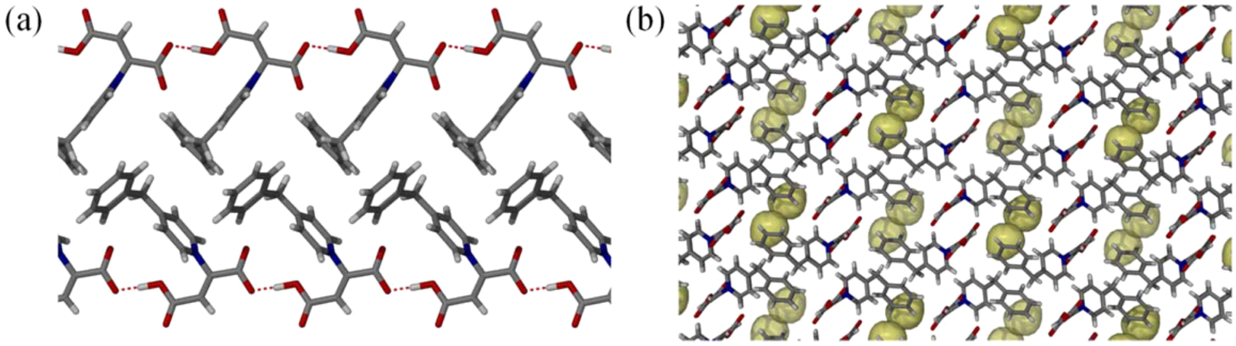

Figure 2. Packing in Form I. (a) Hydrogen-bonded chains of zwitterions. (b) Packing diagram viewed along [010], with voids shown in yellow (voids mapped using MsRoll[29] with a probe radius of 1.5 Å).

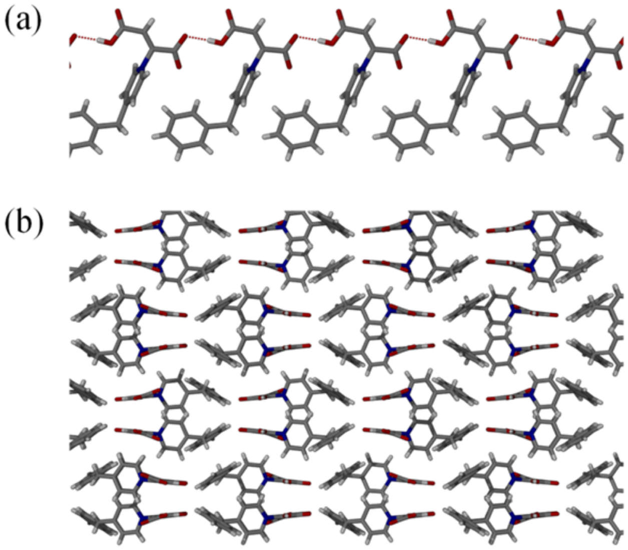

Figure 3. (a) Hydrogen-bonded chains in Form II. (b) Packing in Form II viewed down [010].

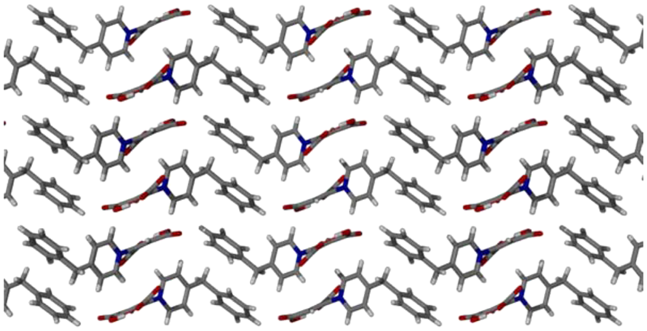

Figure 4. Packing of Form III viewed along [010].

neighboring zwitterions (Figure 6b). TG analysis shows a 13.4% weight loss commencing at approximately 85 °C, which correlates well with the mass loss expected for one-half of a dioxane molecule per zwitterion (calculated mass loss = 13.45%).

The solvate including benzene ($\mathbf{1}_{\mathrm{Benz}}$) is isostructural to $\mathbf{1}_{\mathrm{Diox}}$. When these two structures are overlaid using Mercury[30] (Figure 7a), it is clear that the conformation of the zwitterion in the two structures is essentially identical. The guest molecules occupy the same position in the two structures, but they have different orientations in the pockets. There do not appear to be any significant intermolecular interactions between the host and the guest in $\mathbf{1}_{\mathrm{Benz}}$ (as were observed for $\mathbf{1}_{\mathrm{Diox}}$) but, rather, a size−shape match that allows the benzene molecule to be included. The pockets occupied by the benzene guests were mapped using a probe radius of 1.5 Å (in MsRoll) and have a volume of 146.8 Å^3 (Figure 7b). TG analysis shows a 12.6% weight loss starting at approximately 50 °C, which corresponds to one-half of a benzene molecule per zwitterion (calculated mass loss for one-half of a benzene = 12.11%).

Crystallization from DCM/MeOH yielded crystals of $\mathbf{1}_{\mathrm{MeOH}}$ on only one occasion. This solvate is isostructural to Form I, but MeOH is included in the void. (Crystallization from pure MeOH yields Form IV, vide supra.) $\mathbf{1}_{\mathrm{MeOH}}$ crystallizes in space group $P2_1/n$, with one molecule of **1** and one partially occupied molecule of MeOH in the asymmetric unit. The benzyl moiety of **1** is disordered over two positions of approximately equal occupancy. The methylene bridge angles are 112.54° and 116.16° for the two disordered positions, respectively. The dihedral angles between the aromatic rings are 76.3(2)° and 80.8(3)°. In the single crystal structure, the guest MeOH is just over 25% occupied, but TGA of a bulk sample indicates one molecule of guest per molecule of **1** (mass loss 10.5%; calculated mass loss = 10.15%). This mass loss starts at ambient temperature, so we assume MeOH was lost from the single crystal before data collection. The increase in mass loss above what is expected for one molecule of MeOH per molecule of **1** could be due to surface solvent. We have been unable to verify this experimentally because we were unable to obtain further samples of $\mathbf{1}_{\mathrm{MeOH}}$.

An overlay of the structures of Form I and $\mathbf{1}_{\mathrm{MeOH}}$ is shown in Figure 8. It is clear that the MeOH guests in $\mathbf{1}_{\mathrm{MeOH}}$ reside in what are open pores in Form I, although the void volume in the MeOH solvate is slightly larger (Table 1).

Crystal Structure of Salt 2. Salt **2** crystallizes in monoclinic space group $P2_1/n$ and contains one 4-benzylpyridinium cation and one-half of an acetylenedicarboxylate dianion in the asymmetric unit. The angle at the methylene bridge in the cation is 109.84°, and the carboxylate oxygen atoms are disordered over two positions of equal occupancy. Each dianion hydrogen bonds to two cations, forming a three-component S-shaped adduct (Figure 9a). The three-membered adducts stack in an offset manner along the [010] direction such that the pyridyl moieties are aligned with the acetylene moiety of the next S-shaped unit in the stack. These stacks then pack in a herringbone arrangement perpendicular to the (102) plane (Figure 9b) to form two-dimensional layers. The layers, in turn, pack one on top of another along [100].

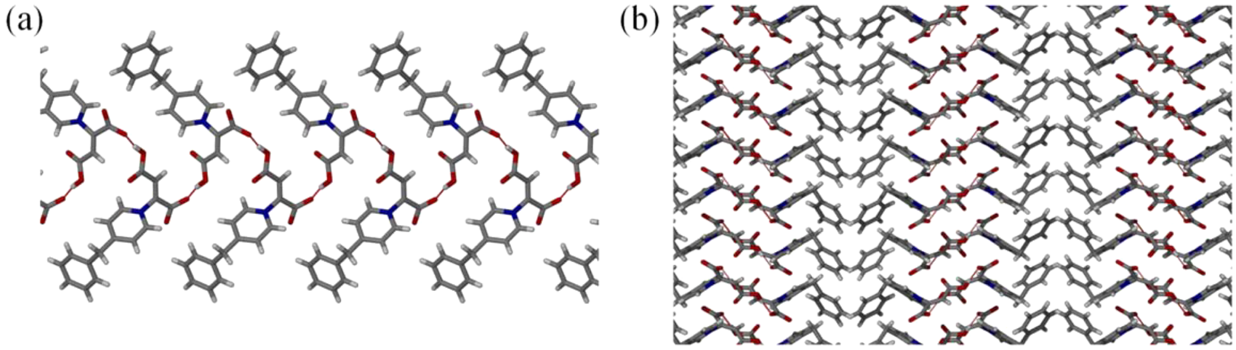

Figure 5. (a) Hydrogen-bonded chain in Form IV viewed down [010]. (b) Packing of IV viewed along [100].

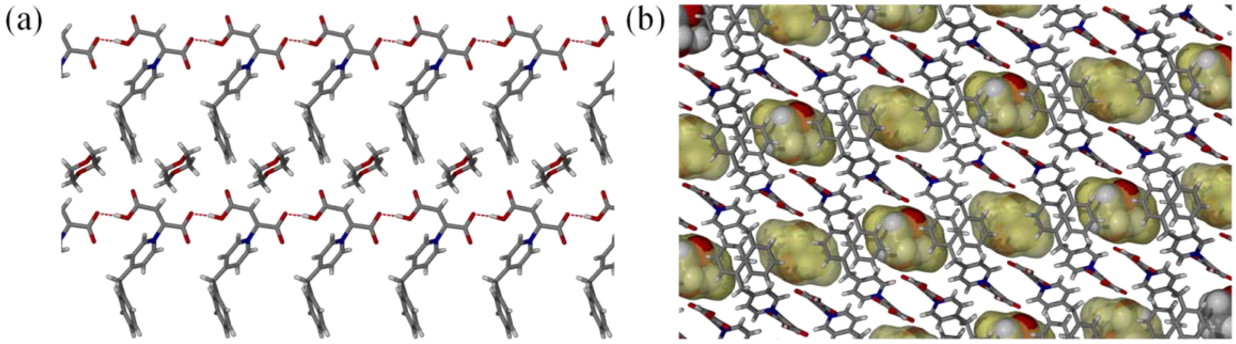

Figure 6. (a) Hydrogen-bonded chains of zwitterions in $\mathbf{1}_{\mathrm{Diox}}$. (b) Solvent pockets viewed down [010], with dioxane guests shown in space filling representation. Void space (contact surface) if the solvent is removed is shown in yellow.

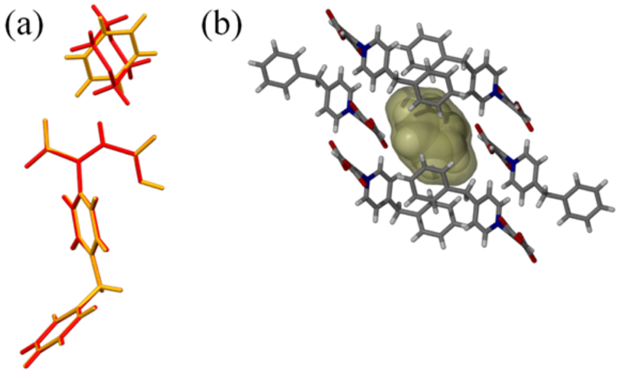

Figure 7. (a) Overlay of the zwitterions from $\mathbf{1}_{\mathrm{Diox}}$ (red) and $\mathbf{1}_{\mathrm{Benz}}$ (yellow). (b) Solvent pocket in $\mathbf{1}_{\mathrm{Benz}}$.

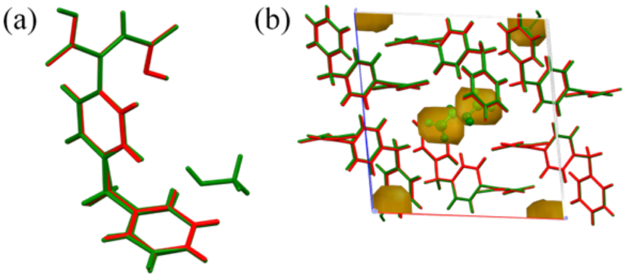

Figure 8. (a) Overlay of the zwitterions in $\mathbf{1}_{\mathrm{MeOH}}$ (green) and Form I (red). (b) Overlay of the packing of $\mathbf{1}_{\mathrm{MeOH}}$ (green) and Form I (red) viewed down [010]. The calculated voids in Form I are shown in yellow, with the MeOH guest molecules of $\mathbf{1}_{\mathrm{MeOH}}$ shown in green ball-and-stick model. Voids were (in this instance) calculated in Mercury[30] using a probe radius of 1.2 Å.

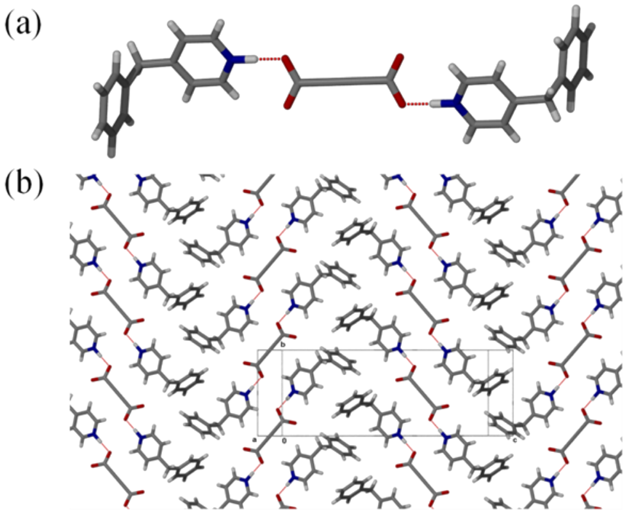

Figure 9. (a) S-shaped hydrogen-bonded units formed in salt **2**. (b) Packing of **2** viewed along (102).

Relationship between the Zwitterion and the Salt. Both zwitterion **1** and salt **2** are obtained by mixing ADC and 4BP in solution (Scheme 1). At first, it seemed that synthesis of zwitterion **1** was not reproducible, as, on some occasions, salt **2** was obtained. It seemed possible that one of the products would be a kinetic product, so the effect of temperature on the product of the reaction was assessed.

Reflux of a 1:1 molar ratio of ADC and 4BP at 75 °C in THF favors nucleophilic addition of the pyridyl to the alkyne moiety, resulting in the isolation of Form IV of zwitterion **1**. Salt **2** could be reproducibly obtained by heating the reaction mixture until the components were dissolved and then placing the vial in the refrigerator (−9 °C) to crystallize. It seems clear that the zwitterion is the thermodynamic product of this reaction, whereas the salt is the kinetic product.

Refluxing salt **2** with additional ADC or refluxing just salt **2** under the same conditions (THF at 75 °C) also yields Form IV of the zwitterion. Refluxing ADC and 4BP in THF at 63 °C gave a mixture of zwitterion Forms I and IV, whereas reflux at 45 °C gave Form I. This indicates that, while the zwitterion is the thermodynamic product of the reaction between ADC and 4BP, the particular solid-state form that is obtained is temperature-dependent.

Mechanochemical reaction of a 1:2 molar ratio of ADC and 4BP, both neat and liquid-assisted (dioxane, benzene, acetone), yields salt **2**.

Transformation between the Forms of 1. The observation of so many solid-state forms of **1** prompted the question of whether conversion between these various forms would be possible. Our first question was whether conversion between Form I and the dioxane or benzene solvates was possible. In order to test this, Form I was exposed to vapors of the solvents or immersed directly in the solvent in question.

When Form I is immersed in dioxane or benzene, the crystals remain unchanged after 6 days. However, after 10 days in dioxane, or exposed to dioxane vapor, both PXRD and TGA show that the crystals of Form I have converted to $\mathbf{1}_{\mathrm{Diox}}$ (see Supporting Information for data). For complete conversion from Form I to the dioxane solvate, a 13% mass loss is expected for TGA. After 10 days immersed in dioxane, the powdered sample shows a mass loss of approximately 12%, indicating almost complete conversion. Powdered Form I exposed to dioxane vapor shows only a 4% mass loss after 10 days, indicating that conversion in this case is much slower. The same experiments were attempted with benzene; however, no significant uptake of benzene had occurred after 10 days.

In order to further investigate the uptake of dioxane by Form I, crystals of Form I immersed in dioxane were photographed for several days. After 1.5 days, the crystals were still Form I. After 2 days, the crystals started to darken (Figure 10). After 10 days, the crystals were completely dark and did not diffract. It is clear from these experiments that uptake of dioxane by Form I does not proceed in a single-crystal-to-single-crystal fashion. The resulting material retains its crystallinity, as is evident from PXRD (see Supporting Information), but no single crystals suitable for X-ray diffraction experiments remain.

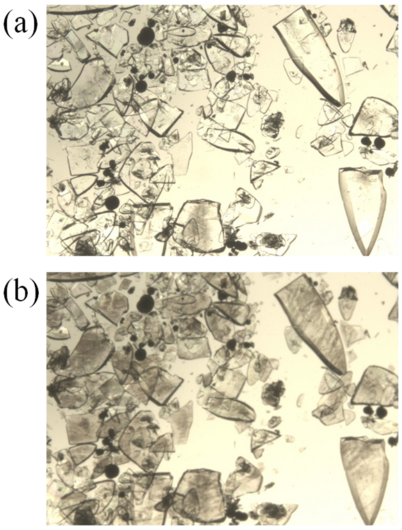

Figure 10. Images of crystals of Form I immersed in dioxane (a) at the start of the experiment and (b) after 2 days.

The conversion of $\mathbf{1}_{\mathrm{Diox}}$ to Form I was also investigated. Crystals of $\mathbf{1}_{\mathrm{Diox}}$ exposed to the air for an extended period (10 days) showed partial conversion from the solvate to Form I. Conversion of $\mathbf{1}_{\mathrm{Diox}}$ to Form I was confirmed using variable-temperature PXRD (VT-PXRD), which shows conversion of the solvate to Form I starting at approximately 60 °C (Figure 11). Because the bulk sample used for PXRD analysis may not have been pure solvate (there may have been some Form I present), this conversion was also studied in a single crystal: a single crystal of $\mathbf{1}_{\mathrm{Diox}}$ was placed on the diffractometer, and a unit cell was determined at 25 °C. The crystal was then heated, and unit cells were determined at various temperatures. Between 60 and 70 °C, the unit cell parameters changed to those of Form I (see Supporting Information for full details). The crystal had deteriorated to such an extent by the end of the experiment that, although a unit cell could be obtained, a full data set could not be collected; conversion of $\mathbf{1}_{\mathrm{Diox}}$ to Form I is also not a single-crystal-to-single-crystal process.

It was also shown using PXRD that the conversion between Form I and $\mathbf{1}_{\mathrm{Diox}}$ is reversible: if Form I is exposed to dioxane, then it converts to $\mathbf{1}_{\mathrm{Diox}}$, and the same sample then converts back to Form I on heating (Supporting Information Figure S14). It is clear from these results that Form I of zwitterion **1** is porous to dioxane. Future work will involve a detailed investigation of the potential of Form I as a porous material.

An examination of the structures of Form I and $\mathbf{1}_{\mathrm{Diox}}$ reveals that the two structures are very closely related. The packing arrangements are essentially the same; however, in the solvate, the hydrogen-bonded chains of zwitterions are slightly farther apart, and the conformation of the zwitterion has changed slightly. The structure of Form I opens up to accommodate the solvent molecules. Figure 12 makes the relationship between the structures clear.

This close relationship between the structures makes it unsurprising that Form I is able to take up dioxane while none of the other forms show conversion to the solvate. What is somewhat surprising is that Form I does not seem to take up other solvents into these voids to any appreciable extent.

In order to confirm this, Form I was immersed in a variety of solvents. The results are given in detail in the Supporting Information, Table S10. In summary, when crystals of Form I

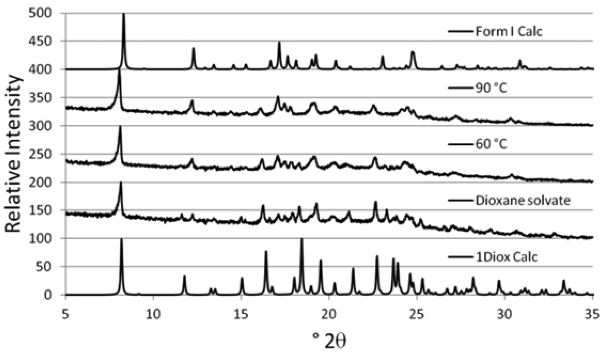

Figure 11. Variable-temperature PXRD showing the conversion of $\mathbf{1}_{\mathrm{Diox}}$ to Form I. The sample was heated from 20 to 90 °C and then cooled to room temperature. PXRD patterns were recorded every 10 °C until 60 °C and then every 5 °C.

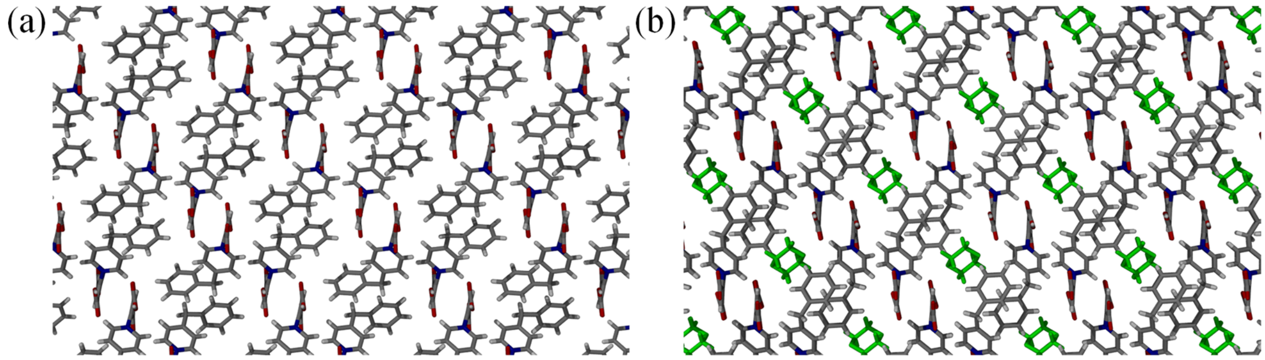

Figure 12. Comparison between the packing in Form I (a) and $\mathbf{1}_{\mathrm{Diox}}$ (b). Dioxane molecules are colored green.

are exposed to smaller guests such as water or methanol, the crystals become opaque or dissolve after 24 h. The microcrystalline product obtained after exposure to water was subjected to PXRD analysis, and it was confirmed that Form I had converted to Form II. This process appears to be irreversible; crystals of Form II were immersed in a variety of solvents, and PXRD confirmed no change when Form II was immersed in acetone, THF, *p*-xylene, benzene, or 1,4-dioxane for 5 days (Supporting Information, Table S11). However, further experiments showed that Form II does convert to Form IV when it is immersed in MeOH (dried on molecular sieves) for 5 days. Dissolving crystals of $\mathbf{1}_{\mathrm{Diox}}$ in a MeOH/water mixture, in the presence of pyrazine, also gave crystals of Form II.

Further investigation into whether any change in form was observed when crystals of Forms I−IV are immersed in various solvents was carried out. These results are detailed in the Supporting Information, Tables S11−S13. It was found that immersing Form I in DMF or methanol yields Form IV. Form II converts to Form IV if it is immersed in MeOH, but it remains unchanged when it is exposed to other solvents. Form III converts to Form IV when it is immersed in a range of solvents. Form IV shows no evidence of conversion to other forms. From these results, it appears that Form IV is the most stable form of **1**.

Thermal Analysis. In order to further investigate the relationships among Forms I−IV, differential scanning calorimetry (DSC) was carried out on the various forms of **1**. Of Form I, II, or IV, none shows any thermal events before decomposition. It seems that conversion between these forms takes place only when it is solvent-mediated.

The DSC of Form III shows a broad endotherm before 100 °C. It seems probable that this is due to conversion to Form IV (vide supra), and this has largely been confirmed by PXRD, although it has proven to be difficult to obtain sufficiently crystalline bulk material to record quality PXRD patterns (see Supporting Information).

DSC of salt **2** shows an endotherm followed by a large exotherm before 100 °C. Observation of a sample using a conventional melting point apparatus, combined with analysis of the TGA data, confirms that this is due to melting followed by decomposition.

DSC and TGA results for Forms I−IV, salt **2**, and the three solvates of **1** are included in the Supporting Information.

The relationship between the various forms is summarized in Figure 13.

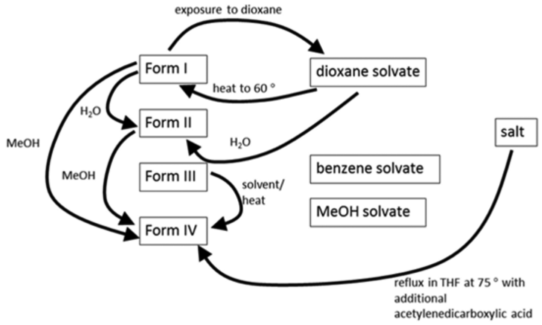

Figure 13. Conversion between the various solid-state forms described in this article.

■ CONCLUSIONS

Reaction between acetylenedicarboxylic acid and 4-benzylpyridine yields two products. The kinetic product, reproducibly obtained from crystallizations at low temperatures, is a salt (**2**), which has been structurally characterized. The thermodynamic product, obtained when the reaction is carried out at higher temperatures, is a zwitterion, (2*Z*)-2-(4-benzylpyridinium-1-yl)-3-carboxy-1-hydroxyprop-2-en-1-olate (**1**). Salt **2** can be converted to **1** by reflux at elevated temperatures.

Four polymorphs and three solvates of **1** have been characterized and described. Form I is porous to dioxane, yielding a dioxane solvate. The MeOH and benzene solvates are also closely related to Form I, but they could not be obtained by exposing Form I to solvent. Conversion between the dioxane solvate and Form II, or Form I and Form II, appears to be solvent-mediated. Crystallization of Form I, III, or IV from a reaction mixture is both temperature- and solvent-dependent. Analysis of the conversions between the various forms suggests that Form IV is the most stable form: Forms I−III all convert to Form IV, but Form IV has shown no evidence of conversion to any of the other forms.

It was anticipated that the unusual shape of zwitterion **1** would result in interesting solid-state supramolecular chemistry. It is clear from the number of forms obtained thus far that this is most certainly the case.

■ EXPERIMENTAL SECTION

Form I of (2*Z*)-2-(4-benzylpyridinium-1-yl)-3-carboxy-1-hydroxyprop-2-en-1-olate (**1**) was obtained by mixing ADC (0.020 g, 0.175 mmol) and 4BP (0.030 g, 0.177 mmol) in either acetone (2 mL), tetrahydrofuran (2 mL), or a mixture of toluene (2 mL) and MeOH (0.5 mL) with stirring and gentle heating. When the components were completely dissolved, the solution was set aside and colorless crystals were afforded after a few days. Form I can also be obtained by exposing the dioxane solvate ($\mathbf{1}_{\mathrm{Diox}}$) to the air for approximately 3 weeks. The dioxane solvate ($\mathbf{1}_{\mathrm{Diox}}$) was obtained by mixing ADC (0.020 g, 0.175 mmol) and 4-benzylpyridine (0.030 g, 0.177 mmol) in 1,4-dioxane (1−2 mL). The solution is colorless when the components first dissolve, but it turns a murky gray and then orange and a dark green; however, the resulting crystals are colorless. The benzene solvate ($\mathbf{1}_{\mathrm{Benz}}$) was obtained by mixing ADC (0.020 g, 0.175 mmol) and 4BP (0.030 g, 0.177 mmol) in a benzene/MeOH (1 mL/0.5 mL) mixture. The colorless crystals are extracted from a dark brown solution. Crystals grown from an acetone/benzene mixture (1:1 molar ratio) gave similar unit cell parameters. The methanol solvate ($\mathbf{1}_{\mathrm{MeOH}}$) was obtained by dissolving ADC (0.044 g, 0.386 mmol) and 4BP (0.075 g, 0.443 mmol) in a dichloromethane/MeOH (4 mL/a few drops) mixture, which was stirred at 60 °C for approximately 5 min and then left to crystallize. Colorless crystals were obtained from a clear pink solution.

Form II[21] was obtained by dissolving $\mathbf{1}_{\mathrm{Diox}}$ (0.020 mg, 0.070 mmol) in H_2O (1 mL) and combining this with pyrazine (0.011 g, 0.137 mmol) or pyridine (0.011 mg, 0.139 mmol) dissolved in MeOH (1 mL), with heating and stirring. The solution was then set aside to crystallize. Form III was obtained by mixing ADC (0.040 g, 0.350 mmol) with 4-benzylpyridine (0.060 g, 0.355 mmol) in a mixture of acetone and *p*-xylene (1:1 molar ratio, 2 mL/4.2 mL) with stirring and gentle heating. The mixture was allowed to cool, and crystals were obtained after a few days. Form IV was obtained from the combination of ADC (0.040 mg, 0.350 mmol) and 4BP (0.060 mg, 0.355 mmol) in MeOH (3 mL) with heating and stirring. A white precipitate was formed within a few hours. This powder was then recrystallized from water; colorless plates were obtained.

Salt **2** was obtained from the reaction of ADC (0.040 g, 0.350 mmol) and 4-benzylpyridine (0.060 g, 0.355 mmol) combined in acetonitrile (2 mL) with gentle heating and stirring. Once all components were dissolved, the solution was allowed to cool to room temperature (or placed in the refrigerator), which yielded colorless crystals after a few days. Crystals were also obtained from acetone, EtOH, and THF when solutions were crystallized at low temperature.

X-ray Diffraction. Single-crystal X-ray intensity data were collected on a Bruker SMART Apex II X-ray diffractometer equipped with a Mo (λ = 0.71073 Å) fine-focus sealed tube and a 0.5 mm MonoCap collimator. The data for $\mathbf{1}_{\mathrm{MeOH}}$ was collected on an Apex Duo Quazer with Incotec Iμs Mo (λ = 0.71073 Å) source. Data were captured with a CCD (charge-coupled device) area detector. Unless stated otherwise, data collections were carried out at 100 K using an Oxford Cryosystems cryostat (700 series Cryostream Plus) attached to the diffractometer. Data collection and reduction were carried out using the Bruker software package APEX2,[31] using standard procedures. All structures were solved and refined using SHELX-2013[32] employed within the X-Seed[33,34] environment. Diagrams were generated using POV-Ray,[35] except for overlays, which were calculated in Mercury.

PXRD patterns were collected using a PANalytical X'Pert Pro diffractometer with Bragg−Brentano geometry using Cu Kα radiation (λ = 1.5418 Å) at 45 kV and 40 mA. Standard samples were run using a reflection-transmission spinner stage using a zero-background sample holder, and samples were spun at 4 revolutions per second. Intensity data were captured with an X'Celerator detector with 2θ scans performed in the range 5−50° with a 0.0167 step size. Some patterns were collected using a Bruker D2 Phaser diffractometer with (Bragg−Brentano geometry) using Cu Kα radiation (λ = 1.5418 Å) at 30 kV and 10 mA. Intensity data were captured with a Lynxeye detector with 2θ scans performed in the range 4−40° with a 0.016° step size. Samples were spun at 30 rpm.

Variable-temperature PXRD patterns were collected using a PANalytical X'Pert Pro diffractometer with a capillary spinner, samples were housed in a 0.5 mm capillary, and the temperature was controlled with an Oxford Cryosystems cryostat between 20 and 90 °C. 2θ scans were collected in the range 5−35°.

Thermal Analysis. Differential scanning calorimetry (DSC) was carried out using a TA Instruments Q20 system under a N_2 gas purge coupled to an RSC cooling unit. Samples were cycled from −20 °C to approximately 200 °C (depending on the T_{dec} obtained from TGA) at a heating rate of 10 °C/min and a cooling rate of 5 °C/min. This was performed using nonhermetically sealed aluminum pans with a pinhole in the lid.

Thermogravimetric analysis was carried out using a TA Instruments Q500 system under a N_2 gas purge using aluminum sample pans at a ramp rate of 10 °C/min.

Images of Form I Crystals Exposed to Dioxane. Crystals of Form I were placed in a short glass vial and covered with approximately 3 mL of 1,4-dioxane. The glass vial was covered with a glass slide to prevent excessive evaporation of the solvent, and the crystals were filmed for 2 days with a Leica Microsystems microscope camera (DFC295). Images were taken every 30 min, and the solvent level was kept constant during the 2 days. After 1.5 days, the crystals had not yet started to darken. SCD analysis showed that all of the crystals selected for SCD analysis were still Form I. Exchange for 1,4-dioxane had, therefore, not yet taken place. By day two, the crystals had started to darken.

In a further experiment, crystals of Form I were photographed for 10 days with a Leica Microsystems microscope camera (DFC295). Images were taken every 30 min for the first 2 days, and for the remaining time, images were taken every hour. The solvent level was kept constant during the 10 days. Between days 2 and 3, the crystals started to darken, and by day 10, the crystals were nearly completely dark. After 10 days, the crystals were removed from the mother liquor for single-crystal X-ray diffraction analysis, but the crystals were very brittle and did not diffract.

■ ASSOCIATED CONTENT

Ⓢ Supporting Information

The Supporting Information is available free of charge on the ACS Publications website at DOI: 10.1021/acs.cgd.5b01238.

TGA, DSC, and PXRD data and selected hydrogen-bonding tables (PDF)

X-ray crystallographic information files (CIF)

CCDC 1420454−1420460 contain the supplementary crystallographic data for this article. These data can be obtained free of charge from The Cambridge Crystallographic Data Centre via www.ccdc.cam.ac.uk/data_request/cif.

■ AUTHOR INFORMATION

Corresponding Author

*Tel.: +27 21 808 3358. E-mail: dhaynes@sun.ac.za.

Notes

Any opinion, findings, and conclusions or recommendations expressed in this material are those of the authors and therefore the NRF does not accept any liability in regard thereto.

The authors declare no competing financial interest.

■ ACKNOWLEDGMENTS

We are grateful to Helene Wahl for collecting the images of Form I crystals. We acknowledge the National Research Foundation of South Africa and Stellenbosch University for funding and the Claude Leon Foundation for a postdoctoral fellowship.

■ REFERENCES

(1) Aakeröy, C. B.; Salmon, D. J. *CrystEngComm* **2005**, *7*, 439−448.

(2) Braun, D. E.; Karamertzanis, P. G.; Arlin, J.-B.; Florence, A. J.; Kahlenberg, V.; Tocher, D. A.; Griesser, U. J.; Price, S. L. *Cryst. Growth Des.* **2011**, *11*, 210−220.

(3) Aakeröy, C. B.; Beatty, A. M.; Helfrich, B. A.; Nieuwenhuyzen, M. *Cryst. Growth Des.* **2003**, *3*, 159−165.

(4) Vishweshwar, P.; McMahon, J. A.; Bis, J. A.; Zaworotko, M. J. *J. Pharm. Sci.* **2006**, *95*, 499−516.

(5) Steed, J. W.; Atwood, J. L. *Supramolecular Chemistry*, 2nd ed.; Wiley: Weinheim, Germany, 2013.
(6) Wahl, H.; Haynes, D. A.; le Roex, T. *CrystEngComm* **2015**, *17*, 1549−1555.
(7) Ducharme, Y.; Wuest, J. D. *J. Org. Chem.* **1988**, *53*, 5787−5789.
(8) Gallant, M.; Phan Viet, M. T.; Wuest, J. D. *J. Org. Chem.* **1991**, *56*, 2284−2286.
(9) Simard, M.; Su, D.; Wuest, J. D. *J. Am. Chem. Soc.* **1991**, *113*, 4696−4698.
(10) Evans, C. C.; Sukarto, L.; Ward, M. D. *J. Am. Chem. Soc.* **1999**, *121*, 320−325.
(11) Russell, V. A.; Etter, M. C.; Ward, M. D. *J. Am. Chem. Soc.* **1994**, *116*, 1941−1952.
(12) Russell, V. A.; Etter, M. C.; Ward, M. D. *Chem. Mater.* **1994**, *6*, 1206−1217.
(13) Russell, V. A.; Evans, C. C.; Li, W.; Ward, M. D. *Science* **1997**, *276*, 575−579.
(14) Swift, J. A.; Reynolds, A. M.; Ward, M. D. *Chem. Mater.* **1998**, *10*, 4159−4168.
(15) Swift, J. A.; Ward, M. D. *Chem. Mater.* **2000**, *12*, 1501−1504.
(16) Yamamoto, A.; Hamada, T.; Hisaki, I.; Miyata, M.; Tohnai, N. *Angew. Chem., Int. Ed.* **2013**, *52*, 1709−1712.
(17) Yamamoto, A.; Hasegawa, T.; Hamada, T.; Hirukawa, T.; Hisaki, I.; Miyata, M.; Tohnai, N. *Chem. - Eur. J.* **2013**, *19*, 3006−3016.
(18) Yamamoto, A.; Hirukawa, T.; Hisaki, I.; Miyata, M.; Tohnai, N. *Tetrahedron Lett.* **2013**, *54*, 1268−1273.
(19) Yamamoto, A.; Uehara, S.; Hamada, T.; Miyata, M.; Hisaki, I.; Tohnai, N. *Cryst. Growth Des.* **2012**, *12*, 4600−4606.
(20) Wahl, H.; Haynes, D. A.; le Roex, T. *Chem. Commun.* **2012**, *48*, 1775−1777.
(21) Loots, L.; Haynes, D. A.; le Roex, T. *New J. Chem.* **2014**, *38*, 2778−2786.
(22) Kumar, S. S.; Nangia, A. *Cryst. Growth Des.* **2014**, *14*, 1865−1881.
(23) Orola, L.; Veidis, M. V.; Sarcevica, I.; Actins, A.; Belyakov, S.; Platonenko, A. *Int. J. Pharm.* **2012**, *432*, 50−56.
(24) Reece, H. A.; Levendis, D. C. *Acta Crystallogr., Sect. C: Cryst. Struct. Commun.* **2008**, *64*, o105−o108.
(25) Nath, N. K.; Kumar, S. S.; Nangia, A. *Cryst. Growth Des.* **2011**, *11*, 4594−4605.
(26) Bolla, G.; Sanphui, P.; Nangia, A. *Cryst. Growth Des.* **2013**, *13*, 1988−2003.
(27) Carter, P. W.; Ward, M. D. *J. Am. Chem. Soc.* **1994**, *116*, 769−770.
(28) Van Der Sluis, P.; Spek, A. L. *Acta Crystallogr., Sect. A: Found. Crystallogr.* **1990**, *46*, 194−201.
(29) Connolly, M. *Science* **1983**, *221*, 709−713.
(30) Macrae, C. F.; Bruno, I. J.; Chisholm, J. A.; Edgington, P. R.; McCabe, P.; Pidcock, E.; Rodriguez-Monge, L.; Taylor, R.; van de Streek, J.; Wood, P. A. *J. Appl. Crystallogr.* **2008**, *41*, 466−470.
(31) *APEX II, SAINT, and SADABS*; Bruker AXS Inc.: Madison, WI, 2012.
(32) Sheldrick, G. M. *Acta Crystallogr., Sect. A: Found. Crystallogr.* **2008**, *64*, 112−122.
(33) Atwood, J. L.; Barbour, L. J. *Cryst. Growth Des.* **2003**, *3*, 3−8.
(34) Barbour, L. J. *J. Supramol. Chem.* **2001**, *1*, 189−191.
(35) *POV-Ray for Windows*, version 3.6.1a.icl8.win32; Persistence of Vision Pty. Ltd., 2003.

DOI: 10.1021/acs.cgd.5b01238
Cryst. Growth Des. XXXX, XXX, XXX−XXX